Inversion of the Cis Geometry Requirement for Cytotoxicity in Structurally Novel Platinum(II) Complexes Containing the Bidentate N,O-Donor Pyridin-2-yl-acetate

Ulrich Bierbach,[†,‡] Michal Sabat,[§] and Nicholas Farrell*[,†]

Department of Chemistry, Virginia Commonwealth University, Richmond, Virginia 23284, and Department of Chemistry, University of Virginia, Charlottesville, Virginia 22901

Received October 26, 1999

Water soluble platinum(II) complexes have been synthesized that contain the N,O-chelate pyridin-2-yl acetate (PyAc) as a novel structural motif in platinum antitumor complexes. The *trans*-platinum complex *trans*-[PtCl(PyAc-*N*,*O*)(NH_3)] (**2**) (N-donors are trans) and its isomer *cis*-[PtCl(PyAc-*N*,*O*)(NH_3)] (**4**) (*N* trans to Cl) were prepared from *trans*-[$PtCl_2$((NH_3)(PyAcH)]·H_2O (**1**·H_2O) and *cis*-[$PtCl_2$(NH_3)(PyAcMe) (**3**), respectively, employing the bidentate ligand as its methylester (PyAcMe). **2** and **4** are readily formed from the respective dichloro species, even at low pH and in the presence of extra chloride, indicating a high thermodynamic stability of the PyAc chelate ring. **1**·H_2O and **2**−**4** were characterized by ^{1}H NMR and IR spectroscopy and elemental analyses. The solid-state structure of **2** was determined: triclinic, $P\bar{1}$ (no. 2), with $a = 8.170(2)$ Å, $b = 9.274(3)$ Å, $c = 7.374(2)$ Å, $\alpha = 108.68(2)°$, $\beta = 113.27(2)°$, $\gamma = 74.40(2)°$, $V = 479.7(6)$ Å^3, $Z = 2$. The six-membered metallacyclus in **2** adopts a "boat" form, allowing a strainless coordination of platinum. The most promising cytotoxic properties in the above series of compounds have been established for **2** (and **1**, which rapidly transforms into **2** at 37 °C and neutral pH). Preliminary ID_{50} values were 0.88 and 1.26 μM, respectively, in cisplatin-sensitive L1210 leukemia. Both compounds proved to be cross-resistant to the clinical drug. Reactions of **2** and **4** with 5′-guanosine monophosphate (5′-GMP) under physiological conditions gave the monofunctional adducts *trans*- and *cis*-[Pt(5′-GMP-*N7*)(PyAc-*N*,*O*)(NH_3)] (**I** and **II**). Chelate-bound carboxylate was not replaced by guanine-N7 when an excess of nucleotide was applied (NMR). In an analogous reaction, **2** reacts with the oligonucleotide *d*(TCGT) [5′-T(1)-C(2)-G(3)-T(4)-3′] to give the adduct *d*(TCGT)-*N7*(3)-Pt(PyAc-*O*,*N*)(NH_3) (**III**), which was characterized by a combination of total correlation spectroscopy, double-quantum-filtered correlation spectroscopy, nuclear Overhauser effect spectrometry, and rotating-frame Overhauser enhancement spectroscopy experiments. Binding of the [Pt(PyAc-*N*,*O*)(NH_3)]$^+$ fragment to N7 of G(3) causes an increase of N-type character of the T(4) and G(3) deoxyribose residues relative to the unplatinated sequence, while those of T(1) and C(2) remain S-type. An internucleotide nuclear Overhauser effect between H6(4) and H2′(3) indicates stacking between guanine and the 3′-thymine base. The most striking feature proved to be the pronounced upfield shift and broadening of the ^{1}H NMR signals assigned to the base protons H5 and H6 in **III**. Magnetization transfer between H5(2) and H3 of pyridine suggests that this effect is caused by base−base interactions involving the planar ligand on platinum, which must be situated on the 5′ face of guanine. Possible implications for the DNA binding and cytotoxic effect of the compounds are discussed.

Introduction

Despite the widely established use of cisplatin, *cis*-[$PtCl_2$(NH_3)$_2$], and carboplatin, [Pt(CBDCA)(NH_3)$_2$] (CBDCA = 1,1-cyclobutanedicarboxylate) (Chart 1), in the treatment of certain cancers,[1] there is a continued interest in the design of structurally novel platinum compounds that show antitumor activity equivalent or complementary to that of the clinical drugs.[2] The fact that transplatin, *trans*-[$PtCl_2$(NH_3)$_2$] (Chart 1), was found to be therapeutically inactive has been considered a paradigm for the structure−activity relationships (SAR) of platinum(II) antitumor compounds.[3] We have reported earlier that the presence of a planar ligand such as pyridine or quinoline (e.g., in *trans*-[$PtCl_2$(NH_3)(quinoline)], Chart 1) dramatically enhances the in vitro cytotoxicity of the trans geometry.[4,5] This finding clearly

Chart 1

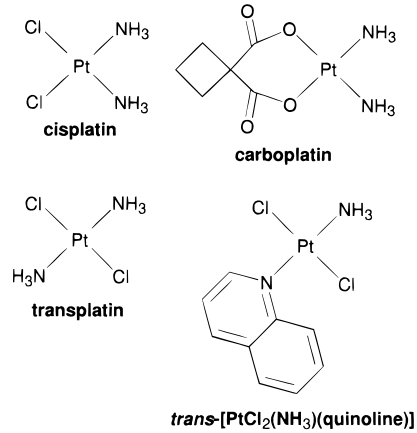

* To whom correspondence should be addressed. E-mail: nfarrell@saturn.vcu.edu. Fax: (804) 828-8599.
† Virginia Commonwealth University.
‡ Current address: Department of Chemistry, Wake Forest University, Winston-Salem, NC 27109.
§ University of Virginia.

(1) (a) Abrams, M. J.; Murrer, B. A. *Science* **1993**, *261*, 725. (b) Kelland, L. R.; Clarke, S. J.; McKeage, M. J. *Platinum Met. Rev.* **1992**, *36*, 178.
(2) Farrell, N. *Cancer Invest.* **1993**, *11*, 578.

10.1021/ic991259p CCC: $19.00 © 2000 American Chemical Society
Published on Web 04/07/2000

demonstrates that the classical SAR do not adequately describe the range of potentially useful platinum drugs.

The biological activity of such "nonclassical" *trans*-platinum complexes has been discussed in terms of both an overall altered affinity toward biologically relevant (N^6 and S^7) nucleophiles and unique DNA binding modes.[8] Classical dichloroplatinum(II) species form monofunctional adducts on DNA, which subsequently transform into bifunctional DNA cross-links[9] (either intrastrand or interstrand). Incubations of *trans*-[$PtCl_2$(NH_3)(quinoline)] with calf thymus DNA for 48 h show that ca. 34% of all covalent DNA−platinum adducts remain monofunctional.[8] Conformational changes in globally platinated DNA caused by this compound[8] are reminiscent of those of the 1,2 intrastrand (GG) cross-link, the most frequently formed[10] and structurally well-characterized (NMR,[11,12] X-ray[13]) lesion of cisplatin. Molecular mechanics calculations suggest that the structural alterations in double-stranded DNA may be ultimately produced by the monofunctional adduct, with quinoline partially intercalating into the base stack on the 5′ face of platinated guanine.[8] Similar drug−DNA interactions and structural effects have been established for the alkylating/intercalating agent aflatoxin B_1.[14] DNA unwinding caused by ethidium-linked platinum complexes[15] has also been related to this type of "pseudobifunctional" binding mode. An analogous lesion induced by nonclassical *trans*-platinum that mimics the major cisplatin adduct may produce similar biological effects. Furthermore, it has been demonstrated that the replacement of an ammine ligand in *trans*-[$PtCl_2$(NH_3)$_2$] with quinoline increases the rate of bifunctional *interstrand* adduct formation and changes the cross-link specificity of the *trans*-platinum geometry from purine−pyrimidine (GC, transplatin-like[16]) to purine−purine (GG, cisplatin-like[17]). Both monofunctional and readily formed bifunctional interstrand adducts may contribute to the cytotoxic properties of *trans*-[$PtCl_2$(NH_3)(quinoline)].

The lack of solubility of the above "nonclassical" *trans*-platinum species has been put forward to explain their limited bioavailability and, consequently, low in vivo activity.[18] Thus, the initial goal of the present synthetic approach was to overcome the poor water solubility of complexes of the type *trans*-[$PtCl_2$(NH_3)L] (L = planar ligand), while retaining the trans orientation of NH_3 and the planar base and the electroneutrality of the square-planar entity. This was achieved with the anionic N,O-chelating ligand pyridin-2-yl-acetate (PyAc), which introduces a carboxylate donor cis to the planar ligand. The unexpected trans geometry requirement for cytotoxicity in this system and the binding mode in reactions with nucleic acid constituents imply that *trans*-[PtCl(PyAc-*N*,*O*)(NH_3)] (**2**), a new cytotoxic transplatin derivative, produces its biological activity via the "pseudobifunctional" mechanism not accessible to the analogous cis isomer (**4**).

Experimental Section

Materials and Supplies. Pyridin-2-yl-acetic acid methylester[19] (PyAcMe) was prepared from pyridin-2-yl-acetic acid hydrochloride (Aldrich) according to standard esterification methods.[20] Cisplatin (*cis*-[$PtCl_2$(NH_3)$_2$]) and K[$PtCl_3$(NH_3)]·H_2O were synthesized as described earlier.[21,22] 5′-Guanosine monophosphate (5′-GMP) was employed as its disodium salt (Sigma). The tetradeoxyribonucleotides *d*(TCGT) and *d*(TGCT) were synthesized by The Midland Certified Reagent Company (Midland, TX) using cyanoethylphosphoramidite protecting group chemistry. Both oligomers were obtained as yellowish, dried sodium salts, which were repurified prior to use (vide infra). All other reagents and solvents were obtained from common vendors and used as supplied.

Synthesis of (*SP*-4-1)-Amminedichloro(pyridin-2-yl-acetic acid-*N*)platinum(ii) (1). A mixture of 1.791 g (5.96 mmol) of cisplatin and 2.700 g (17.88 mmol) of pyridin-2-yl-acetic acid methylester in 100 mL of water was heated at 90−100 °C for 2 h. To the solution was added 18 mL of concentrated HCl, and heating was continued for 5 h. Concentration of this mixture to a volume of 20 mL and storage at 4 °C afforded **1**·H_2O as a bright-yellow crystalline solid, which was filtered off and washed with EtOH and Et_2O. Yield 1.290 g (50%). ^{1}H NMR (300 MHz, DMF-d_7): δ 3.53 (crystal water), 4.20 (br, 3 H, NH_3), 4.99 (s, 2 H, CH_2), 7.43 (t, 1 H, H5), 7.68 (d, 1 H, H3), 7.96 (t, 1 H, H4), 8.92 (d, 1 H, H6), 13.06 (br, 1 H, CO_2H). IR (KBr): ν(CO) 1716 cm^{-1}. Anal. Calcd for $C_7H_{12}N_2Cl_2O_3Pt$: C, 19.19; H, 2.76; N, 6.39. Found: C, 19.29; H, 2.50; N, 6.30.

Synthesis of (*SP*-4-2)-Amminechloro(pyridin-2-yl-acetato-*N*,*O*)-platinum(ii) (2). To a solution of 1.000 g of Na_2HPO_4 in 50 mL of water (pH ∼9) were added 0.500 g (1.14 mmol) of **1**·H_2O, and the mixture was heated at 50 °C until all of the platinum complex was dissolved (less than 5 min). **2** precipitated spontaneously as fine, off-white needles, which were collected after the reaction mixture had cooled to room temperature and finally recrystallized from 10^{-2} M HCl. Yield 0.290 g (66%) of pale-yellow prisms. ^{1}H NMR (300 MHz, DMF-d_7): δ 4.07 (s, 1 H, CH_2), 4.53 (br, 3 H, NH_3), 7.50 (t, 1 H, H5), 7.62 (d, 1 H, H3), 8.08 (t, 1 H, H4), 8.91 (d, 1 H, H6). IR (KBr): ν(CO) 1647 cm^{-1}. Anal. Calcd for $C_7H_9N_2ClO_2Pt$: C, 21.90; H, 2.36; N, 7.30. Found: C, 21.88; H, 2.36; N, 7.25.

Synthesis of (*SP*-4-3)-Amminedichloro(pyridin-2-yl-acetic acid methylester-*N*)platinum(ii) (3). Typically, a mixture of 0.151 g (1 mmol) of pyridin-2-yl-acetic acid methylester and 0.376 g (1 mmol) of K[$PtCl_3$(NH_3)]·H_2O was stirred in 3 mL of water at room temperature for 30 min. As the potassium salt dissolved, a yellow precipitate formed, which was filtered off, washed with EtOH and Et_2O, and dried in a vacuum. Yield 0.354 g (82%). ^{1}H NMR (300 MHz, DMF-d_7): δ 3.80 (s, 3 H, CH_3), 4.29 (br, 3 H, NH_3), 4.78−5.25 (m, 2 H, CH_2, AB system—see Results and Discussion), 7.49 (t, 1 H, H5), 7.74 (d, 1 H, H3), 8.01 (t, 1 H, H4), 9.14 (d, 1 H, H6). IR (KBr): ν(CO) 1724 cm^{-1}. Anal. Calcd for $C_8H_{12}N_2Cl_2O_2Pt$: C, 22.13; H, 2.78; N, 6.45. Found: C, 22.08; H, 2.31; N, 6.25.

Synthesis of (*SP*-4-3)-Amminechloro(pyridin-2-yl-acetato-*N*,*O*)-platinum(ii) (4). A suspension of 0.240 g (0.55 mmol) of **3** in 10 mL of 10^{-2} M H_2SO_4 was stirred at 65 °C for 2 h until a light-yellow solution had formed. After concentration of the solution, **4** precipitated as a pale-yellow microcrystalline solid, which was filtered off, washed with EtOH and Et_2O, and dried in a vacuum. Yield 0.103 g (48%). ^{1}H

(3) Farrell, N. *Transition Metal Complexes as Drugs and Chemotherapeutic Agents*; Ugo, R., James, B. R., Eds.; Kluwer: Dordrecht, The Netherlands, 1989; Chapters 2 and 3.
(4) Farrell, N.; Ha, T. T. B.; Souchard, J.-P.; Wimmer, F. L.; Cros, S.; Johnson, N. P. *J. Med. Chem.* **1989**, *32*, 2241.
(5) Van Beusichem, M.; Farrell, N. *Inorg. Chem*. **1992**, *31*, 634.
(6) Bierbach U.; Farrell, N. *Inorg. Chem*. **1997**, *36*, 3657.
(7) Bierbach, U.; Farrell, N. *JBIC, J. Biol. Inorg. Chem.* **1998**, *3*, 570.
(8) Zákovská, A.; Nováková, O.; Balkarová, Z.; Bierbach, U.; Farrell, N.; Brabec, V. *Eur. J. Biochem.* **1998**, *254*, 547.
(9) Bancroft, D. P.; Lepre, C. A.; Lippard, S. J. *J. Am. Chem. Soc.* **1990**, *112*, 6860.
(10) Fichtinger-Schepman, A. M.; van der Veer, J. L.; den Hartog, J. H.; Lohman, P. H.; Reedijk, J. *Biochemistry* **1985**, *24*, 707.
(11) Yang, D.; van Boom, S. S. G. E.; Reedijk, J.; van Boom, J. H.; Wang, A. H.-J. *Biochemistry* **1995**, *34*, 12912.
(12) Gelasco, A.; Lippard, S. J. *Biochemistry* **1998**, *37*, 9230.
(13) Takahara, P. M.; Frederick, C. A.; Lippard, S. J. *J. Am. Chem. Soc*. **1996**, *118*, 12309.
(14) Johnston, D. S.; Stone, M. P. *Biochemistry* **1995**, *34*, 14037.
(15) Keck, M. V.; Lippard, S. J. *J. Am. Chem. Soc.* **1992**, *114*, 3386.
(16) Brabec, V.; Leng, M. *Proc. Natl. Acad. Sci. U.S.A.* **1993**, *90*, 5345.
(17) Huang, H.; Zhu, L.; Reid, B. R.; Drobny, G. P.; Hopkins, P. B. *Science* **1995**, *270*, 1842.
(18) Farrell, N. *Met. Ions Biol. Syst.* **1996**, *32*, 603.
(19) Woodward, R. B.; Kornfeld, E. C. In *Organic Syntheses*; Wiley: New York, 1955; Collective, Vol. 5, p 413.
(20) Harrison, I. T.; Harrison, S. *Compendium of Organic Synthetic Methods*; Wiley: New York, 1971; p 273 and literature cited therein.
(21) Dhara, S. C. *Indian J. Chem.* **1970**, *8*, 193.
(22) Abrams, M. J.; Giandomenico, C. M.; Vollano, J. F.; Schwartz, D. A. *Inorg. Chim. Acta* **1987**, *131*, 3.

NMR: δ 4.07 (s, 2 H, CH_2), 4.69 (br s, 3 H, NH_3), 7.50 (t, 1 H, H5), 7.69 (d, 1 H, H3), 8.13 (t, 1 H, H4), 8.84 (d, 1 H, H6). IR (KBr): ν(CO) 1633 cm^{-1}. Anal. Calcd for $C_7H_9N_2ClO_2Pt$: C, 21.90; H, 2.36; N, 7.30. Found: C, 22.05; H, 2.15; N, 7.25.

Nucleotide Binding Studies. **2** and **4** were incubated with 1 and 2 equiv of 5′-GMP at a platinum concentration of 5 mM at 40 °C for 24 h. A phosphate buffer (0.067 M KH_2PO_4/Na_2HPO_4) was used to maintain a pH of 6.5. The solutions were finally evaporated to dryness and the residues lyophilized twice from 1 mL of 99.96% D_2O and redissolved in D_2O for the ^{1}H NMR investigations. The NMR samples were then kept at 40 °C for another 24 h and reexamined by ^{1}H NMR spectroscopy.

The crude batches of *d*(TCGT) and *d*(TGCT) were purified and desalted on a 300 mm × 10 mm Sephadex G10 column (FPLC system equipped with a UV detector operating at 280 nm and a conductivity cell; eluent water, pH 7.3; flow rate 0.20 mL min^{-1}) before the incubations with **2**. In parallel experiments, 3 mg (2.5 mmol) of each tetranucleotide was reacted with 0.96 mg (2.5 mmol) of **2** in 1 mL of 99.996% D_2O at 40 °C for 96 h. The pH* (uncorrected pH meter reading for D_2O solutions) was adjusted to 6.5 using 0.1 M DCl and NaOD solutions. ^{1}H NMR spectra of these mixtures were taken every 12−16 h to monitor the progress in platinum binding and to determine the completeness of the reaction. Where necessary, an excess of complex was added to complete platination. The mixtures were lyophilized and the residues redissolved in 200 μL of water. Salt and excess of platinum were removed from the aqueous solutions (pH adjusted to 7.3) on a 100 mm × 10 mm Sephadex G10 column using the above conditions. Final lyophilization of the product fractions yielded 1.25 mg of **III** and 2.1 mg of **IV**, which were further studied (in 99.999% D_2O) by NMR spectroscopy.

X-ray Data Collection and Structure Determination. Single crystals of **2** were grown by slow evaporation of an aqueous solution at room temperature. All X-ray measurements were carried out on a Rigaku AFC6S diffractometer using Mo Kα radiation. Calculations were performed using the program packages TEXSAN 5.0 and teXan 1.7.[23] Unit cell dimensions were determined by applying the setting angles of 25 independent high-angle reflections. Three standard reflections were monitored during the data collection, which showed no significant variance. Reflex intensities were corrected for absorption by applying ψ scans of several reflections with the transmission factors ranging from 0.51 to 1.00. The structure was solved by Patterson and Fourier methods followed by full-matrix least-squares refinement with anisotropic displacement parameters for all non-hydrogen atoms. All hydrogen atoms were found in difference Fourier maps and included as fixed contributions to the refinement. The final difference map showed the highest peak of 1.76 e/Å^2 in the vicinity of the Pt atom. Relevant crystallographic data are summarized in Table 1. Selected bond lengths and angles of **2** are given in Table 2. Tables of positional parameters, thermal displacement parameters, a complete list of bond lengths and angles, intermolecular distances, and torsional angles have been deposited in Supporting Information.

Physical Measurements. One-dimensional ^{1}H NMR spectra of **1**−**4** (64 transients) and **I**−**II** (128 transients) were recorded at 294 K on a Varian Gemini-300 instrument operating at 300 MHz, equipped with a variable temperature unit. Chemical shifts were referenced to TMS except for D_2O solutions, where DSS (4,4-dimethyl-4-silapentane-sulfonic acid) was used as an internal standard. Two-dimensional NMR data sets for D_2O solutions of **III** (ca. 2 mM) were acquired with a spectral window of 7994 Hz on a Varian Unity-Plus-500 instrument at 500 MHz using the following conditions: (i) for total correlation spectroscopy (TOCSY), acquisition temperature 5 °C, 1024 complex points in t_2, 300 t_1 experiments (128 transients), 1 s recycle delay, 80 ms spin-lock mixing time; (ii) for nuclear Overhauser effect spectrometry (NOESY), acquisition temperature 5 °C, 1024 complex points in t_2, 300 t_1 experiments (128 transients), 3 s recycle delay, 400 ms mixing time; (iii) for rotating-frame Overhauser enhancement spectroscopy (ROESY), acquisition temperature 5 °C, 1024 complex points in t_2, 256 t_1 experiments (128 transients), 3 s recycle delay, 400 ms mixing time; (iv) for double-quantum-filtered correlation spectroscopy (dqf-COSY), acquisition temperature 22 °C, 1024 complex points in t_2, 600 t_1 experiments (128 transients), 0.9 s recycle delay. All data sets were multiplied with apodization functions (90° phase-shifted sine−bell except for the ROESY data, where a Kaiser function was applied) and zero-filled to final matrices of 2048 × 2048 data points before Fourier transformation. The HDO signal was eliminated (except for the dqf-COSY data) by applying convolution-based solvent suppression. The final matrices were referenced to the internal HDO signal, using values obtained for an external standard [δ_{HDO} vs DSS standard at pH 7: 4.961 (5 °C), 4.786 (22 °C)]. One-dimensional spectra at 500 MHz were taken at both temperatures with the same spectral window and 64 scans. All data were processed employing FELIX.[24]

The ^{195}Pt NMR spectrum of **I** was taken on a General Electric QE-300 spectrometer at 64.5 MHz (293 K, c_{Pt} = 20 mM, spectral width 125 000 Hz, relaxation delay 500 μs, 60 000 transients). IR spectra were recorded on a Perkin-Elmer 1600 FTIR instrument. Elemantal analyses were performed by QTI, Whitehouse, NJ.

Cytotoxicity. The in vitro cytotoxicity of **1**−**4** discussed in this paper was determined from 72 h incubations of the drugs at 37 °C with both wild-type murine L1210 and cell lines resistant to cisplatin using a standard assay described previously.[25] **1**−**4** were dissolved in saline. ID_{50} values were calculated as a percentage of control cells from logarithmic plots of complex concentration vs cell counts and represent an average of three (for **1** and **2**) or two (for **3** and **4**) individual experiments.

Table 1. Crystal Data for **2**

space group	$P\bar{1}$ (no. 2)
a, Å	8.170(2)
b, Å	9.274(3)
c, Å	7.374(2)
α, deg	108.68(2)
β, deg	113.27(2)
γ, deg	74.40(2)
V, Å^3	479.7(6)
fw	383.70
D_{calc}, g cm^{-3}	2.66
empirical formula	$C_7H_9N_2ClO_2Pt$
Z	2
abs coeff, cm^{-1}	150.3
temp, °C	−120
λ, Å	0.71069
$R(F_o)^a$	0.034
R_w [b]	0.044

[a] $R = \sum(||F_o| - |F_c||)/\sum|F_o|$. [b] $R_w = [(\sum w(||F_o| - |F_c||)^2/\sum w(|F_o|)^2]^{1/2}$.

Table 2. Selected Bond Lengths and Angles with Standard Deviations for **2**

	Bond Length (Å)		
Pt−Cl	2.274(3)	Pt−O1	2.205(7)
Pt−N1	2.002(8)	Pt−N2	2.037(8)
O1−C8	1.33(1)	O2−C8	1.20(1)
	Bond Angle (deg)		
Cl−Pt−O1	175.8(2)	Cl−Pt−N1	92.2(2)
Cl−Pt−N2	90.6(3)	O1−Pt−N1	89.5(3)
O1−Pt−N2	87.8(3)	N1−Pt−N2	176.2(3)
Pt−O1−C8	118.1(6)	Pt−N1−C2	119.2(6)
Pt−N1−C6	120.7(7)		

Results and Discussion

Synthetic Aspects. Schemes 1 and 2 depict the synthetic pathways that lead to *trans*-[PtCl(PyAc-*N*,*O*)(NH$_3$)] (**2**) and its geometric isomer *cis*-[PtCl(PyAc-*N*,*O*)(NH$_3$)] (**4**), respectively. The *trans*-dichloro species, **1**, is formed under strongly acidic

(23) TEXSAN 5.0 and teXsan 1.7: Single-Crystal Structure Analysis Software; Molecular Structure Corp.: The Woodlands, TX, 1989, 1995.

(24) *FELIX 97.0*; Biosym Technologies: San Diego, CA, 1997.

(25) Farrell, N.; Qu, Y.; Hacker, M. P. *J. Med. Chem.* **1990**, *33*, 2179.

Scheme 1

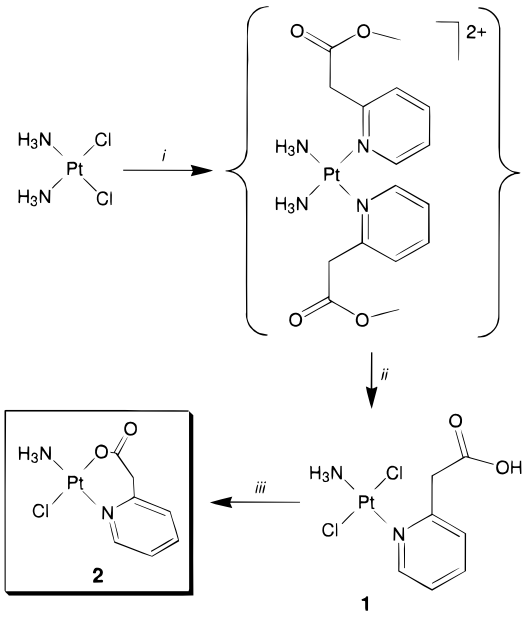

Scheme 2

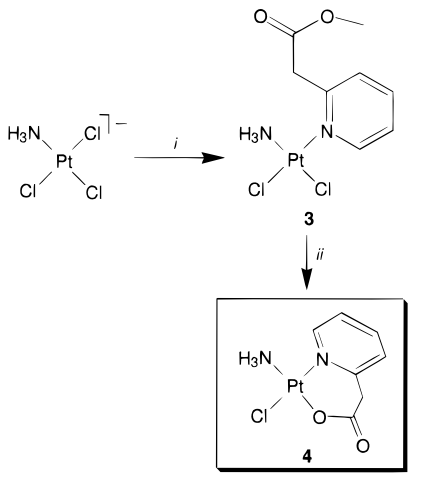

conditions in the presence of chloride. A nitrogen ligand in the dicationic intermediate is labilized at low pH and subsequently substituted by chloride (Scheme 1), which, in turn, directs the second chloro ligand into the trans position because of the relative order of trans effects ($Cl^- >$ am(m)ine).[26] Similarly, the synthesis of **3** (Scheme 2) utilized the mutual labilization of the trans oriented chloro ligands in $[PtCl_3(NH_3)]^-$ for the stereospecific introduction of a planar base. Both preparations used the didentate ligand in its O-protected form (i.e., the corresponding methylester (PyAcMe)). Formation of the N,O-chelates was achieved via the isolable intermediate dichloro forms *trans*-$[PtCl_2(NH_3)(PyAcH)]\cdot H_2O$ (**1**·H_2O) and *cis*-$[PtCl_2(NH_3)(PyAcMe)]$ (**3**) at neutral and moderately acidic (ester cleaving) pH, respectively. The remarkably facile displacement of chloride in **1** and **3** by carboxylate under the above conditions (e.g., in 10^{-2} M HCl) is in contrast to the situation for "classical"

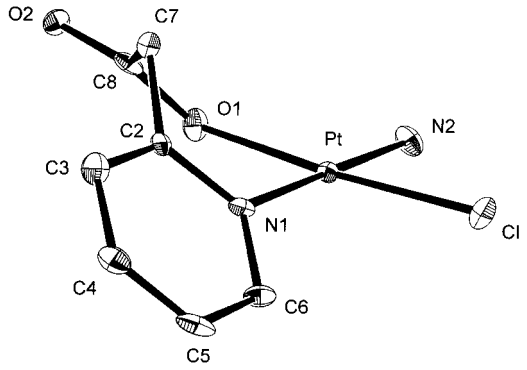

Figure 1. Molecular structure of **2** in the crystal. Hydrogen atoms have been omitted for clarity.

oxygen-based leaving groups in platinum antitumor complexes; bidentate malonate in [Pt(en)(malonato-*O*,*O*′)] (en = ethylenediamine) is readily displaced by chloride and dissociates from the metal at low pH.[27] The pronounced chelate effect observed for pyridin-2-yl-acetate not only controls the formation of the six-membered metallacycles in **2** and **4** but also profoundly affects the target binding properties of platinum in reactions with nucleobase nitrogen (vide infra).

Characterization of 1−4. The novel platinum(II) complexes **1**−**4** were characterized by ^{1}H NMR spectra, IR spectra, and elemental analyses (see also Experimental Section). For **2**, an X-ray structure determination was performed. In the solid state, **2** consists of discrete, neutral complex molecules (Figure 1) that are packed with weak intermolecular hydrogen bonding interactions (O1···N2 2.96(1) Å, O2···N2 3.29(1) Å). In **2**, platinum exhibits a square-planar [N_2OCl] environment with the expected trans coordination of the N-donors. The Pt−N, Pt−O, and Pt−Cl distances are in the usual range observed for divalent platinum.[26] Bond angles around the metal only marginally deviate from 90° and 180°, respectively, which suggests a strainless coordination of the PyAc ligand. The six-membered chelate ring adopts a boatlike, folded conformation, which is characterized by an angle of ca. 70° between planes through Pt−N1−C2−C7 and Pt−O1−C8−C7. The ^{1}H NMR spectrum of **2** (and **4**) in DMF-d_7 shows a sharp singlet for the methylene protons (C7), suggesting a high degree of structural flexibility of the N,O-chelate and rapid interconversion of different conformations in solution. This is in contrast to **3** where an AB system is observed for these protons. In this case the unexpected nonequivalence of the CH_2 protons is due to the prochirality of the methylene group. If rotation about the Pt−N_{py} bond is slow on the NMR time scale, the methylene protons in **3** become diastereotopic. This is in contrast to compound **1**, which exhibits a plane of symmetry (C_s). Intramolecular ammine−carboxylate (NH···O) hydrogen bonding involving mutually cis oriented ammine and PyAcMe and repulsive forces between the ester group on pyridine and the ligands on platinum may contribute to this effect. When the sample (in DMF-d_7) temperature is increased to 70 °C, the AB pattern shows considerable line broadening, which may indicate an increase in intramolecular dynamic exchange rates. The coalescence temperature, however, could not be established because of thermal decomposition of **3** at high temperatures. A similar case of an unusually high barrier of rotation has been reported previously for platinum-bound bulky quinoline ($T_{coalesc}$ = 75 °C, $\Delta G^{\ddagger} > 80$ kJ mol^{-1}).[6]

The improved solubility (ca. 4−5 mmol L^{-1}) of the target compound **2** in water, compared to analogous complexes *trans*-

(26) Roundhill, D. M. Platinum. In *Comprehensive Coordination Chemistry*; Wilkinson, G., Ed.; Pergamon: Oxford, U.K., 1987.

(27) Cutbush, S. D.; Kuroda, R.; Neidle, S.; Robins, B. *J. Inorg. Biochem.* **1983**, *18*, 213.

Table 3. Cytotoxicity Data[a] for **1**−**4** in L1210 Leukemia Cells

compound	ID_{50}, μM	
	L1210/0	L1210/DDP
1·H_2O	1.26	12.5 (9.9)[b]
2	0.88	14.2 (16.1)
3	4.30	>20 (4.7)
4	20	>20
cis-[$PtCl_2(NH_3)_2$], cisplatin[c]	0.33	9.22 (28)
	0.43[d]	11.0 (26)[d]
trans-[$PtCl_2(NH_3)_2$], transplatin[c]	15.7	22.0 (1.4)
cis-[$PtCl_2(NH_3)$(quinoline)][c]	0.48	2.75 (5.73)
trans-[$PtCl_2(NH_3)$(quinoline)][c]	0.51	1.35 (2.7)

[a] L1210/0 is the cisplatin-sensitive and L1210/DDP the cisplatin-resistant cell line. [b] Value in parentheses is the resistance factor $ID_{50,resistant}/ID_{50,sensitive}$. [c] Reference 5. [d] Average of ≥24 experiments.

[$PtCl_2(NH_3)$L] (L = planar N-donor), may be ascribed to the hydrogen-bond acceptor properties of the carboxylate group. A similar increase in solubility of the platinum complex is observed when replacing both chloroligands in cisplatin with a dicarboxylate ligand (e.g., in clinical carboplatin).[28]

Cytotoxicity. The most striking feature of chelate complexes **2** and **4** proved to be their distinct cytotoxicities, as monitored by cell-growth inhibition experiments in murine L1210 leukemia. The precursor complexes **1** and **3** were also included in the study. Preliminary data show that in vitro the trans isomer **2** is comparably cytotoxic to cisplatin itself and gave ID_{50} values (Table 3) in the cisplatin-sensitive cell line (L1210/0) similar to those previously established for *trans*-[$PtCl_2(NH_3)$(quinoline)].[5] Unlike the quinoline-based complex, **2** shows drastically reduced cytotoxicity in cisplatin-resistant cells and has to be considered cross-resistant to the clinical drug. The precursor of **2** (i.e., the *trans*-dichloro complex **1**) exhibits a behavior similar to that of **2**, as could be expected from the reactivity of the complex. **1** rapidly transforms into **2** with a half-life of less than 30 min under conditions that mimic the in vitro experiments (^{1}H NMR spectroscopy; 37 °C; phosphate buffer, pH 7.4; 0.1 M NaCl). Thus, **1** may be considered a short-lived pro-drug that generates **2**, the species that ultimately reacts with target DNA in a manner that obviously produces cisplatin-like biological behavior. The cis isomer **4** proved to be inactive, while its precursor, **3**, was found to be moderately active in L1210/0. **3** maybe considered a direct cisplatin derivative, with one ammine ligand in the classical drug being substituted by PyAcMe. A compound structurally related to **3**, *cis*-[$PtCl_2(NH_3)$(2-methylpyridine)], has been reported recently and is undergoing clinical trials.[29]

Previous studies have demonstrated that certain types of nonleaving groups, such as planar nitrogen bases (vide supra) or *E*-iminoethers,[30] can turn *trans*-platinum complexes into cytotoxic agents that may be, in some cases, even more potent than their cis analogues. The present pair of geometric isomers **2** and **4**, however, represents the first example of a trans geometry *requirement* for an active platinum complex.

Nucleotide Binding. To contribute to an understanding of the distinct biological activities of **2** and **4**, both complexes were reacted with 5′-guanosine monophosphate (5′-GMP) in a simple model reaction to monitor the affinity of platinum to guanine-N7, the preferred binding site for platinum-based drugs.[31] (The choice of these experiments is based on the assumption that the difference in cytototoxicities established for the cis and trans isomer lies at the DNA level.) The reactions were carried out at 40 °C near physiological pH. When reacted at a 1:1 molar ratio with 5′-GMP, **2** and **4** form the monofunctional adducts *trans*-[Pt(5′-GMP-*N7*)(PyAc-*N*,*O*)(NH_3)] (**I**) and *cis*-[Pt(5′-GMP-*N7*)(PyAc-*N*,*O*)(NH_3)] (**II**) (Figure 2), in accordance with integral intensity ratios of pyridine and nucleotide ^{1}H NMR signals. Platinum coordination to the N7 position of the guanine base has been established for **I** and **II**. ^{1}H NMR spectra of both species show signals for the H8 base protons shifted to lower field relative to those of the unplatinated nucleobase. Furthermore, these signals do not show a downfield shift in spectra taken at low pH (data not shown). This is in contrast to the free nucleotide where this effect is observed because of protonation of unplatinated N7 ($pK_a = 2.4$).[32] Selected NMR data for **I** and **II** are in Table 4. Platination of 5′-GMP changes the sugar pucker of the D-ribose in **I** and **II** from S-type (C2′-endo/C3′-exo) to N-type (C3′-endo/C2′-exo) as indicated by the characteristic decrease in the three-bond coupling constants, $^3J_{H1'-H2'}$.[33] The resonances of pyridine H3−H6 in **I** appear upfield of the corresponding signals for **II**, a consequence of the former base protons being exposed to the ring current effect of cis oriented guanine. This effect is most pronounced for H6 ($\Delta\delta_{I-II} = 0.71$ ppm), which shows the closest spatial proximity to the nucleobase in **I**. Thus, the ^{1}H chemical shifts of the pyridine protons are a useful probe for adduct constitution and can rule out cis−trans isomerizations for nucleotide binding to the (pure) geometric isomers **2** and **4**. **I** and **II** show no reaction with a second equivalent (and larger excess) of nucleotide at prolonged incubation periods. No new set of signals is observed in the aromatic and sugar proton regions that would indicate the formation of a bifunctional adduct. The H8 and H1′ signals for free 5′GMP in these mixtures are observed at 8.21 and 5.94 ppm ($^3J = 6.3$ Hz), respectively. Further evidence for the proposed structures depicted in Figure 2 was provided by ^{195}Pt NMR spectroscopy. A ^{195}Pt resonance for **I** in D_2O (ca. 20 mM, pH 6.6) at −1930 ppm (vs $[PtCl_6]^{2-}$ standard) proves to be consistent with a [N_3O] environment[34] of the divalent metal center.

The outcome of these binding studies indicates that carboxylate, incorporated into the six-membered PyAc chelate ring, cannot be displaced by guanine nitrogen under biologically relevant conditions and thus has to be considered a nonleaving group. The inertness toward a second nucleotide binding step is probably caused by both the steric hindrance produced by the planar groups in **I** and **II** in associative substitution reactions and the chelate effect of the N,O-donor. A combination of both effects obviously disfavors bis(guanine) substitution even more dramatically than in analogous *trans*-dichloro complexes, such as *trans*-[$PtCl_2(NH_3)$(quinoline)]. For the latter complex the second guanine binding step proceeds ca. 2.5 times more slowly than for classical transplatin.[6] A similar preference for chloride displacement over chelate opening has been reported recently for platinum(II) complexes containing iminodiacetate (a N,O,O ligand that forms five-membered chelate rings).[35] Finally, the above observations strongly suggest that **2** and **4** form monofunctional adducts on target DNA and that these should persist on the time scale of cellular events critical to the antitumor

(28) McKeage, M. J. *Drug. Saf.* **1995**, *13*, 228.
(29) Holford, J.; Raynaud, F.; Murrer, B. A.; Grimaldi, K.; Hartley, J. A.; Abrams, M.; Kelland, L. R. *Anti-Cancer Drug Des.* **1998**, *13*, 1.
(30) Coluccia, M.; Nassi, A.; Loseto, F.; Boccarelli, A.; Mariggio, M. A.; Giordano, D.; Intini, F. P.; Caputo, P.; Natile, G. *J. Med. Chem.* **1993**, *36*, 510.
(31) Pinto, A. L.; Lippard, S. J. *Biochim. Biophys. Acta* **1985**, *780*, 167.
(32) Dijt, F. J.; Canters, G. W.; den Hartog, J. H. J.; Marcelis, A. T. M.; Reedijk, J. *J. Am. Chem. Soc.* **1984**, *106*, 3644.
(33) Okamoto, K.; Behnam, V.; Viet, M. T. P.; Polissiou, M.; Gauthier, J.-Y.; Hanessian, S.; Theophanides, T. *Inorg. Chim. Acta* **1986**, *123*, 3.
(34) Appleton, T. G.; Hall, J. R.; Ralph, S. F. *Inorg. Chem.* **1985**, *24*, 4685.
(35) Lin, F.-T.; Shepherd, R. E. *Inorg. Chim. Acta* **1998**, *271*, 124.

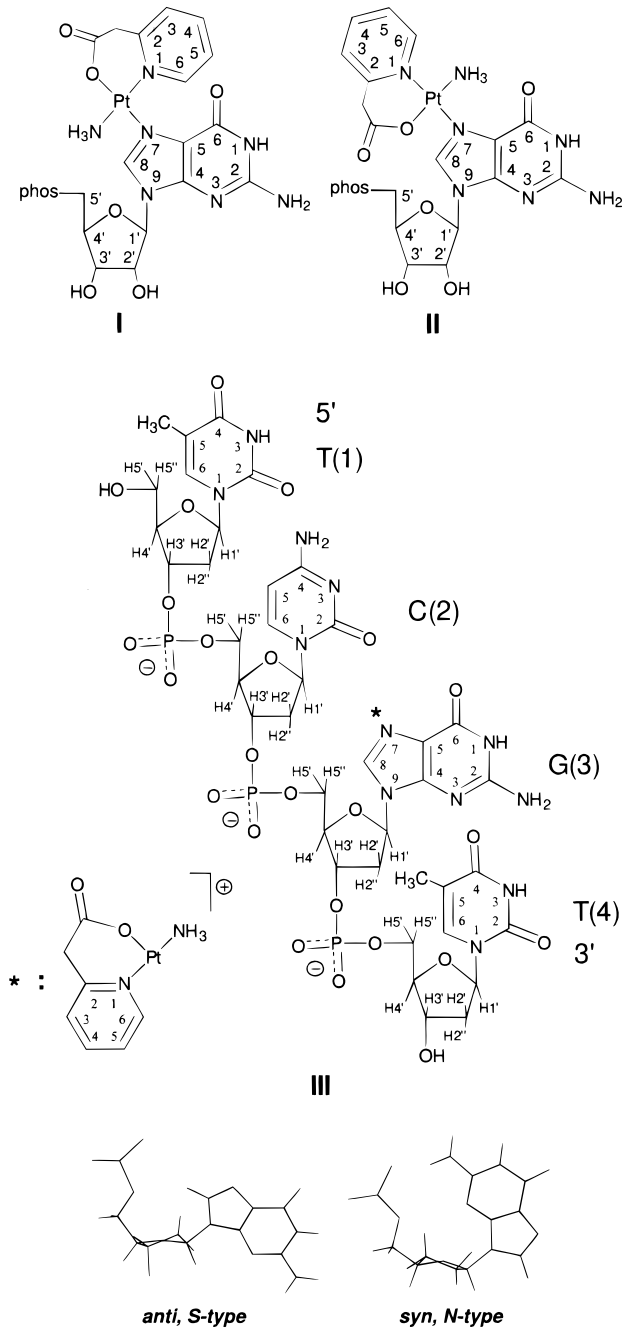

Figure 2. Molecular structures of the monofunctional adducts *trans*- and *cis*-[Pt(5′-GMP-*N7*)(PyAc-*N*,*O*)(NH$_3$)] (**I**, **II**) and [*d*(TCGT)-*N7*(*3*)-Pt(PyAc-*O*,*N*)(NH$_3$)] (**III**) with atom numbering. Binding of the [Pt(PyAc-*N*,*O*)(NH$_3$)]$^+$ fragment to guanine-N7(3) in **III** is indicated by an asterisk for clarity. The *d*(G) residue was chosen to visualize two major conformational features that were used to define the structure of **III** in solution: (i) the two principal sugar puckers, defined by endocyclic torsional angles of the furanose ring, are S-type (C2′-endo, C3′-exo) and N-type (C3′-endo, C2′-exo); (ii) the orientation of the nucleobase with respect to the sugar moiety is defined by the torsional angle χ about the C1′−N glycosidic bond (O4′−C1′−N1−C2 for pyrimidines, O4′−C1′−N9−C4 for purines). Syn refers to a conformation with H8$_{purine}$ or H6$_{pyrimidine}$ situated above the sugar moiety ($\chi = 0 \pm 90°$). In the anti conformation, these protons point away from the sugar and produce a short H8/H1′ and H6/H1′ contact, respectively ($\chi = 180 \pm 90°$).

action of platinum (DNA replication). Therefore, both **2** and **4** should not act as cross-linking agents, and **2**, a monofunctionally binding, active trans complex, must produce its cytotoxicity by a mechanism different from that of bifunctional cisplatin.

Table 4. ^{1}H NMR Data (Downfield and H1′ Region) for the Adducts *trans*-[Pt(5′-GMP-*N7*)(PyAc-*N*,*O*)(NH$_3$)] (**I**) and *cis*-[Pt(5′-GMP-*N7*)(PyAc-*N*,*O*)(NH$_3$)] (**II**)

	I δ, ppm (mult/*J*, Hz)	**II** δ, ppm (mult/*J*, Hz)
H8[a]	8.96 (s)	8.90 (s)
H1′ [b]	6.05 (d/5.0)	6.07 (d/4.2)
H3	7.57 (d/7.8)	7.62 (d/7.7)
H4	7.98 (t/7.8)	8.07 (t/7.7)
H5	7.23 (t/6.6)	7.53 (t/6.1)
H6	7.89 (d/6.0)	8.60 (d/5.0)

[a] 8.21 ppm in free 5′-GMP. [b] 5.94 ppm, $^3J = 6.3$ Hz in free 5′-GMP.

2D NMR Characterization of the Adduct [*d*(TCGT)-*N7*(*3*)-Pt(PyAc-*O*,*N*)(NH$_3$)] (III). It has been demonstrated previously that monofunctional platinum(II) complexes that contain a planar intercalating nonleaving group produce conformational changes in DNA (e.g., unwinding of supercoiled plasmid) different from those effected by simple am(m)ine complexes, such as [PtCl(am)$_3$]$^+$ [am = NH$_3$; (am)$_3$ = diethylenetriamine, dien].[8] To effectively interact with the DNA base stack in a monofunctional adduct (or intermediate), the planar nitrogen base on the metal needs to be cis oriented to the leaving group that is to be replaced with nucleobase nitrogen. This has been demonstrated for monofunctional major groove adducts formed by *trans*-[PtCl$_2$(NH$_3$)(quinoline)] in B-DNA using molecular mechanics calculations.[8] The latter complex and related compounds show a high affinity to alternating purine−pyrimidine (GC) sequences on DNA,[36] consistent with an intercalative binding mode.[37] Stacking of quinoline with adjacent nucleobases should preferentially occur on the 5′ face of platinated guanine (i.e., with nucleobases in the 5′ direction on the platinated strand). Precedence exists for this particular small-molecule-DNA interaction: aflatoxin B$_1$ alkylates N7 of guanine and produces stacking of its planar moiety with the adjacent 5′-cytosine of the same strand.[14] Thus, a logical extension of our NMR studies on mononucleotide binding of **2** (vide supra) was the use of oligonucleotides to examine possible interactions between the pyridinyl ligand and pyrimidine bases flanking the platination site.

Two tetranucleotides, *d*(TCGT) [5′-T(1)C(2)G(3)T(4)-3′, containing a 5′-cytosine base] and *d*(TGCT) [5′-T(1)G(2)C(3)-T(4)-3′, containing a 3′-cytosine base], were chosen for the present study and incubated with **2** for 96 h at 40 °C. From the reaction mixtures we isolated the adducts [*d*(TCGT)-*N7*(*3*)-Pt(PyAc-*O*,*N*)(NH$_3$)] (**III**, Figure 2) and [*d*(TGCT)-*N7*(*2*)-Pt(PyAc-*O*,*N*)(NH$_3$)] (**IV**, structure not shown), respectively. In both cases, **2** forms monofunctional adducts, as evidenced by integral ^{1}H NMR signal intensity ratios in agreement with incubations using 5′-GMP. The typical shift of the H8 resonance of the guanine base in both cases of ca. 0.5−0.6 ppm to lower field relative to that of the free oligonucleotides indicates platination of the G(3)-N7 and G(2)-N7 positions, respectively (Figure S1 of Supporting Information). Covalent binding of platinum to C(2)-N3 and C(3)-N3 was not observed.

A comparison of the downfield regions in the NMR spectra of **III** and **IV** (Figure S1 of Supporting Information) shows critical differences in the line shape and chemical shifts for H5 and H6 of the respective cytosine bases adjacent to the platinated guanine bases. In spectra taken at 21 °C, the H5 signal in **III** is observed at 5.70 ppm, ca. 0.3 ppm upfield of that in free

(36) Bierbach, U.; Qu, Y.; Hambley, T. W.; Peroutka, J.; Nguyen, H. L.; Doedee, M.; Farrell, N. *Inorg. Chem.* **1999**, *38*, 3535.
(37) Neidle, S. *DNA Structure and Recognition*; Rickwood, D., Ed.; IRL Press: Oxford, U.K., 1994.

Table 5. ^{1}H Chemical Shift Assignments[a] (ppm) for Nonexchangeable Protons in [*d*(TCGT)-*N7*(*3*)-Pt(PyAc-*O*,*N*)(NH_3)] (**III**)

	chemical shift			
proton	T(1)	C(2)	G(3)	T(4)
H1′	6.10	6.31	6.25	6.27
H2′	2.20[b]	2.71[b]	2.73	2.31
H2″	2.43[b]	2.88[b]	2.73	2.31
H3′	4.68	5.00	4.92	4.56
H4′	4.12	4.31	4.41	4.11
H5′[c]	3.72	4.01	4.12	4.06
H5″[c]	3.76	4.05	4.20	4.13
H5		5.56		
H6	7.55	7.58		7.69
H8			8.58	
CH_3	1.80			1.71

PyAc H3, 7.47 H4, 7.86 H5, 7.10 H6, 7.61 CH_2, *d*

[a] Based on TOCSY and NOESY spectra taken at 5 °C. [b] Assignments based on relative cross-peak intensities for H1−H2′ and H1′−H2″ in ROESY/NOESY spectra; see text. [c] Shifts in ABM systems may be interconverted. [d] Not assigned because of peak overlap.

d(TCGT) under the same conditions. In addition, this signal, which represents a sharp doublet (^3J = 7.0 Hz) in unmodified *d*(TCGT), is almost unrecognizably broadened in **III**. A similar effect is observed for H6, which had to be identified and assigned with the help of ^{1}H−^{1}H correlated spectra (vide infra) because of spectral overlap in the aromatic region of the spectrum. Signal broadening is also observed for the ribose proton H1′ of the cytosine residue. For the pyridine protons H3−H6, chemical shift effects similar to those observed in the GMP adduct, **I**, indicate the expected cis orientation of the planar ligands on platinum. While this effect is also observed for **IV**, H5 and H6 of the cytosine [C(3)] base give sharp doublets at 5.95 and 7.82 ppm, respectively (Figure S1 of Supporting Information). Unlike for **III**, these signals appear slightly downfield of those in free *d*(TGCT).

The distinct temperature dependence of the H5 and H6 signals in **III** can be taken as evidence for altered base−base interactions in the oligonucleotide sequence. On lowering the sample temperature from 40 to 5 °C, H5 and H6 are shifted upfield by $\Delta\delta$ 0.23 and 0.10 ppm, respectively, with the signals sharpening at low temperatures. The pyridine protons are affected in a similar way but to a lesser extent ($\Delta\delta$ 0.05−0.1 ppm). Taken together, the spectral features observed suggest that platinum-binding to the N7 position of G(3) in the sequence *d*(TCGT) causes a change in intramolecular exchange rates associated with the dynamic behavior (e.g., altered stacking−destacking equilibria) of the 5′ adjacent C(2) residue. The presence of the [Pt(PyAc-*N*,*O*)(NH_3)]$^+$ fragment in **III** changes $\delta_{H5(2)}$ and $\delta_{H6(2)}$ probably because of the ring current effect of the pyridine ligand. The absence of similar effects for bases flanking G(2) in **IV** (and T(4) in **III**) suggests that pyridine-modified platinum may preferentially interact with the 5′-cytosine base.

2D NMR data sets were acquired for **III** at 500 MHz, including TOCSY, dqf-COSY, NOESY, and ROESY spectra. The complete assignment of all nonexchangeable base and sugar protons (Figure 2, Table 5) was possible from TOCSY and NOESY experiments at 5 °C. Four individual spin systems were detected for the ribose residues in the TOCSY spectrum of **III** (Figure 3). Magnetization transfer between the nucleobase and sugar protons, detected in the NOESY (not shown) and ROESY (Figure 4) spectra, was used to establish intraresidue connectivities. To further distinguish between the T(1) and T(4) residues, the NOESY and ROESY spectra were examined for connectivities along the H1′/H2′/2″(*i*−1) → H8/H6(*i*) (*i* = residue number) pathway;[38] a cross-peak due to a strong NOE between thymine-H6 (7.69 ppm) and guanine-H2′/2″ (2.73 ppm) unambiguously identifies the corresponding thymidine residue as T(4) at the 3′ end of the strand. Furthermore, this NOE is indicative of base stacking between 3′-thymine and guanine.[39] No additional NOEs were observed between protons of adjacent nucleotides in the NOESY and ROESY spectra taken with mixing times of 400 ms, probably because of the high rate of molecular tumbling even at lowered temperatures.

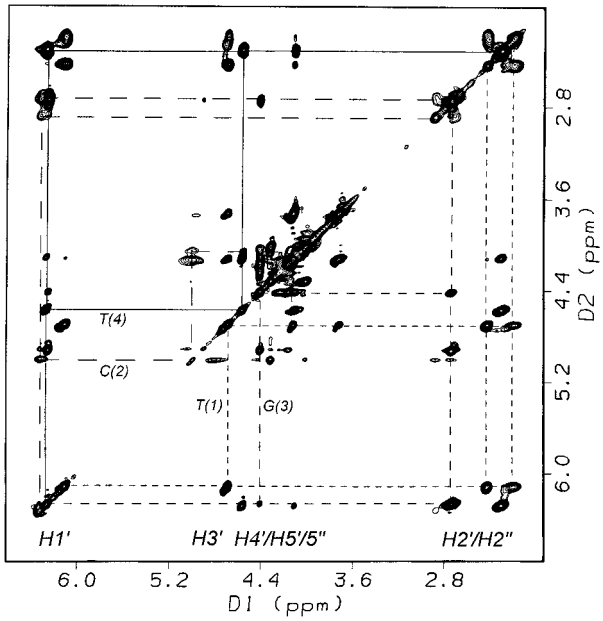

Figure 3. 2D TOCSY spectrum of [*d*(TCGT)-*N7*(*3*)-Pt(PyAc-*O*,*N*)(NH_3)] (**III**) showing connectivities for the spin systems, which are indicated by solid and dashed lines.

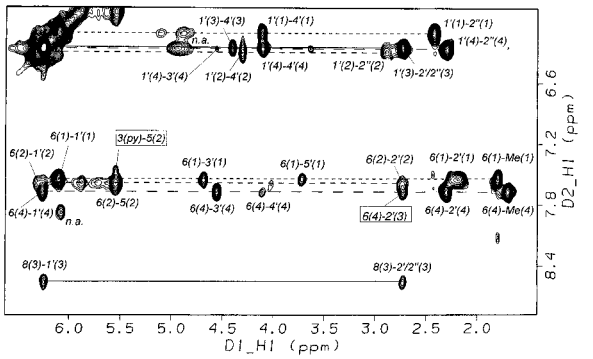

Figure 4. Section of the 2D ROESY spectrum of [*d*(TCGT)-*N7*(*3*)-Pt(PyAc-*O*,*N*)(NH_3)] (**III**) showing cross-peak assignments. Intraresidue cross-peaks are connected as follows: T(1) small dash; C(2) medium dash; G(3) solid line; T(4) large dash. Assignments for interresidue contacts are shown in rectangular boxes. Cross-peaks denoted "*n.a.*" probably result from spectral noise or impurities and were not assigned.

From intraresidue (nucleobase−sugar) through-space contacts and through-bond couplings (^3J between nonexchangeable protons of the ribose moieties), details of the structure of **III** in solution were deduced.

(a) T(4). Two strong cross-peaks due to intranucleotide NOEs between H6(4) and H2′(4) and between H6(4) and H3′(4) and one of weaker intensity for H6−H1′ (Figure 4) are in accordance with the thymine residue of T(4) adopting an anti/high-anti

(38) Evans, J. N. S. *Biomolecular NMR Spectroscopy*; Oxford University Press: Oxford, U.K., 1995; pp 341−391.
(39) Wemmer, D. E.; Chou, S.-H.; Hare, D. R.; Reid, B. R. *Biochemistry* **1984**, *23*, 2262.

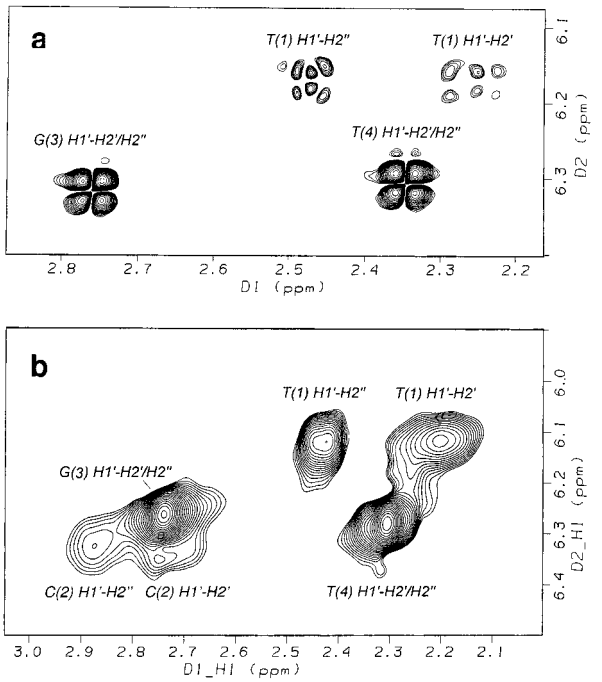

Figure 5. Sections of the 2D dqf-COSY (a) and TOCSY (b) spectrum of [*d*(TCGT)-*N7*(*3*)-Pt(PyAc-*O*,*N*)(NH_3)] (**III**) taken at 22 and 5 °C, respectively, showing cross-peaks resulting from vicinal H1′−H2′/2″ couplings.

glycosidic conformation and an N-type conformation of the ribose (see Figure 2 for definitions[40]). The nature of the sugar pucker is further corroborated by coupling features within the H1′ multiplet. According to a semiquantitative approach by Rinkel and Altona,[41] the population of a particular sugar conformation in a fast S/N equilibrium can be roughly estimated from the sum of three-bond couplings involving H1′. For T(4), $\Sigma^3J_{H1'} = 11.7$ Hz, determined from dqf-COSY (Figure 5a) and 1D spectra taken at 500 MHz, indicates predominantly (60−70%) N-type conformation of the deoxyribose.

(b) G(3). A situation similar to that of T(4) ($\Sigma^3J_{H1'} = 11.5$ Hz) is observed for the ribose conformation of residue G(3). Unambiguous definition of the sugar pucker and base orientation was complicated because of spectral overlap and the coincidence of cross-peaks in the H2′/H2″ region of the 2D spectra. Two strong cross-peaks result from intranucleotide contacts between H8 and the sugar protons H1′ and H2′/2″ and the *absence* of an NOE between H8 and H3′ (Figure 4). These strongly suggest that the increase in N-type sugar character is associated with an anti → syn transition of the guanine base orientation.

(c) C(2). The extraction of structural information from the present NMR data sets proved to be difficult because of signal broadening associated with the slow dynamic exchange observed for this residue. No connectivities could be established for H1′−H2′ and H1′−H2″ in the dqf-COSY spectrum (Figure 5a) taken at 22 °C.[42] Cross-peaks resulting from both couplings, however, are observed in the TOCSY spectrum of **III** obtained at 5 °C (Figure 5b). The corresponding cross-peaks for $^3J_{H1'-H2'}$ and $^3J_{H1'-H2''}$ of almost equal intensity (for a deoxyribose sugar, an increase in N-type character causes a decrease in $^3J_{H1'-H2'}$ and finally a disappearance of the coupling, as can be predicted from the Karplus equation[38]) and a strong NOE between H6 and H2′ (Figure 4) suggest the presence of an S-type ribose conformation and an anti orientation of the pyrimidine base. The initially proposed interaction between the cytosine base and pyridine is supported by the appearance of a (weak) NOE cross-peak resulting from a close contact between H5 of C(2) and H3 of the planar ligand on platinum (Figure 4).

(d) T(1). Both the presence of cross-peaks associated with $^3J_{H1'-H2'}$ and $^3J_{H1'-H2''}$ in the TOCSY and dqf-COSY spectra (Figure 5) and the coupling features extracted from the nicely resolved H2′ and H2″ multiplets ($\Sigma^3J_{H1'} = 15.7$ Hz, $\Sigma^3J_{H2'} = 31.2$ Hz, $\Sigma^3J_{H2''} = 21.3$ Hz) are in accordance with a typical[41] S-type sugar pucker. The NOEs observed for H6 of the 5′-thymine base with H2′ and H1′ (strong) as well as for H3′ and H5′ (weak) result from an overall higher conformational flexibility within this residue. Especially, a less directed orientation of the nucleobase with respect to the C1′−N1 glycosidic bond and free rotation about the C4′−C5′ bond may contribute to this effect. This structural feature, which is in contrast to the situation at the 3′ end of the present oligonucleotide, has been reported before for the bifunctional adduct [*d*(TGGT)-*N7*(2),*N7*(3)-Pt(en)][43] (en = ethylenediamine) and can be attributed to the absence of base stacking between neighboring T(1) and C(2).

In conclusion, platinum coordination to the N7 position of residue G(3) causes a transition from S-type ($\Sigma^3J_{H1'}$ is 14.0−14.5 Hz for all four residues of unplatinated 5′-TCGT-3′) to N-type sugar for T(4) and G(3), with the nucleobases adopting conformations that are best described as part anti and part syn. For T(1) and C(2), S-type sugar puckers persist, which are typically found in right-handed B-type DNA.[38,40] Both the observed stacking between T(4) thymine and G(3) guanine and the interaction between C(2) cytosine and platinum-bound pyridine are only compatible with the latter base being located on the 5′ face of guanine, which, in turn, directs the platinum-based ligand toward residue C(2). The upfield shifts of proton resonances of C(2) in **III** are strongly suggestive of increased base−base interactions involving the pyrimidine base. While analogous signals in the adduct [*d*(CGT)-*N7*(*2*)-Pt(dien)] appear downfield of those in unplatinated *d*(CGT), indicating reduced base−base interactions in the *d*(C)−*d*(G) base stack,[44] pyridine in **III** causes a shift of $\delta_{H5(2)}$ and $\delta_{H6(2)}$ in the opposite direction. Furthermore, the proposed base stacking between cytosine and platinum-bound pyridine reflects the commonly observed enhancement of stacking between N-quarternized (alkylated or metalated) planar, electron-deficient (nucleo)bases.[45] The absence of an interligand NOE between guanine-H8 and pyridine-H6 implies an orientation of the planar bases with the above protons situated on different sides of the square-planar platinum coordination sphere. The AMBER[46] model in Figure 6 (see caption for structural details) visualizes a possible conformation[47] of **III** in solution derived from 2D NMR data.

(40) Saenger, W. *Principles of Nucleic Acid Structure*; Cantor, C. R., Ed.; Springer: New York, 1984; Chapter 2.
(41) Rinkel, L. J.; Altona, C. *J. Biomol. Struct. Dyn.* **1987**, *4*, 621.
(42) Owing to longer rotational correlation times, lines in H1′ and H2′/H2″ multiplets proved to be broad at 5 °C and line widths were on the same order as the coupling constants for the resonances correlated by a given cross-peak. Therefore, the dqf-COSY spectrum was acquired at 22 °C to avoid loss of vicinal coupling information for T(1), G(3), and T(4).
(43) Spellmeyer Fouts, C.; Marzilli, L. G.; Byrd, R. A.; Summers, M. F.; Zon, G.; Shinozuka, K. *Inorg. Chem.* **1988**, *27*, 366.
(44) Van Garderen, C. J.; Altona, C.; Reedijk, J. *Eur. J. Biochem.* **1988**, *178*, 115.
(45) (a) Kawai, H.; Tarui, M.; Doi, M.; Ishada, T. *FEBS Lett.* **1995**, *370*, 193. (b) Bolte, J.; Demuynck, C.; Lhomme, J. *J. Med. Chem.* **1977**, *20*, 1607.
(46) Weiner, S. J.; Kollman, P. A.; Case, D. A.; Singh, U. C.; Ghio, C.; Alagona, G.; Profeta, S., Jr.; Weiner, P. *J. Am. Chem. Soc.* **1984**, *106*, 765.

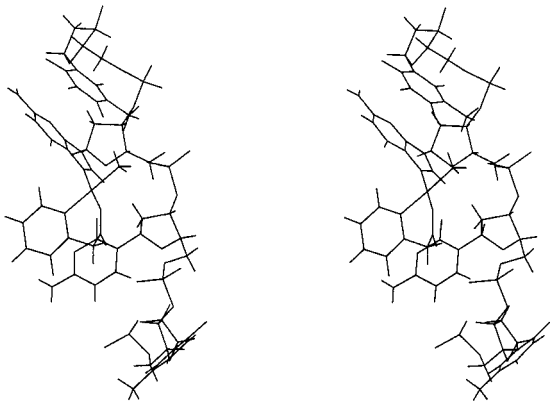

Figure 6. Stereoview of an energy-minimized AMBER model of [*d*(TCGT)-*N7*(*3*)-Pt(PyAc-*O*,*N*)(NH_3)] (**III**). The starting structure was built using geometry constraints based on NMR data. The sequence is presented with the residues oriented 3′ → 5′ from top to bottom. Nonbonded interresidue distances are the following: H5(2)···H3(py) 3.28 Å, H(6)···H2′(3) 2.76 Å, H_3N···OPO_3(3) 2.78 Å, H_3N···O4(4) 2.90 Å. Sugar puckers are S-type for T(1) and C(2) (pseudorotational angles, $P = 110$ and 168°, respectively) and N-type for G(3) and T(4) ($P = -7$ and 13°, respectively). The nucleobases relax into anti orientations with χ in the range 150−177°. Computational details have been deposited as Supporting Information.

Conclusions

The initial goal of the present study was the design of water soluble nonclassical *trans*-platinum complexes that are derived from analogous complexes described earlier, such as *trans*-[$PtCl_2(NH_3)$(quinoline)]. While this was achieved with the introduction of the bidentate ligand pyridin-2-yl acetate, the resulting neutral complex **2** shows greatly altered reactivity with respect to a second binding step to nucleobase nitrogen. This unexpected reactivity feature suggests that **2**, deprived of its bifunctionality because of the lack of chelate opening, should be unable to form bifunctional adducts on DNA. This is in contrast to the structurally related dichloro derivatives. Nevertheless, **2** proves to be as effective as clinical cisplatin at inhibiting L1210 tumor cell growth. From the differences in reactivity and the distinct cytotoxicity profiles established for the pairs of geometric isomers, **2**/**4** and *trans*-/*cis*-[$PtCl_2(NH_3)$-(quinoline)] (Table 3), it can be concluded that the ability of platinum(II) complexes to induce cross-links on DNA is not a prerequisite for producing cytotoxicity. Cisplatin-like biological behavior of "monofunctional" **2** much likely results from an alternative target binding mode (i.e., "pseudobifunctional" covalent/intercalative binding) that ultimately mimics the 1,2 intrastrand cross-link and its impact on DNA topology, protein recognition, and cellular repair.[48] The present NMR study of the DNA binding of **2** using the oligonucleotide *d*(TCGT) supports this view. Despite the structural shortcomings (a flexible single-stranded DNA fragment was chosen to simulate an adduct on a conformationally constrained template, that is, double stranded DNA), this small model provides evidence for an interaction of a planar amine on platinum with an adjacent 5′-cytosine base. Wang and co-workers[49] showed for structurally related *cis*-[$PtCl(NH_3)_2$(4-methylpyridine)]$^+$ bound to a self-complementary heptamer that this kind of 5′ directed stacking interaction may result in disruption of Watson−Crick hydrogen bonding in the base pair adjacent to platinated guanine. From this (structural) point of view, the absence of cytotoxicity observed for *cis*-[PtCl(PyAc-*N*,*O*)(NH_3)] (**4**) may be simply due to the fact that in its monofunctional DNA adduct, the pyridine moiety is oriented trans to the guanine and is unable to interact with the base stack. A similar model has been put forward to explain the inefficacy of structurally related Pt−ethidium compounds at unwinding supercoiled DNA.[15]

The current study also supports the assumption that long-lived monofunctional adducts (intermediates) formed by *trans*-[$PtCl_2(NH_3)$(quinoline)] on DNA constitute potential cytotoxic lesions. The reason for the absence of cross-resistance to cisplatin in L1210 leukemia observed for the latter complex, which is in contrast to the situation for **2**, remains uncertain. However, it may be speculated that both differences in DNA repair and intracellular detoxification mechanisms contribute to this effect. First, the quinoline-based *trans*-dichloro complex forms interstrand cross-links on DNA at a high frequency.[8,16] Cellular repair of this particular lesion, which should not be accessible to **2**, may be less efficient than that of the intrastrand adduct and its pseudobifunctional mimic. Second, cisplatin resistance is often associated with an increased level of endogenous detoxifying, platinum-scavenging thiols.[50] An increase of planar ligand size (quinoline > pyridine) may disfavor a nucleophilic attack by sulfur on the platinum(II) center, thereby enhancing the pharmacological efficacy of the compound.

Regardless of the in vivo activity, currently under investigation, and the clinical success of **2**, the present study provides valuable insight into the general structural requirements for active platinum(II) antitumor complexes as well as new aspects for platinum drug design.

Acknowledgment. This work was supported by grants from The National Science Foundation and The American Cancer Society. We thank Dr. Neel J. Scarsdale for the acquisition of 2D NMR data sets and Dr. Y. Qu for helpful discussions. Thanks are also due to A. Jones, B. Miller, and M. Nguyen for assistance with the synthesis of **1**−**4** and to J. Peroutka for obtaining cytotoxicity data.

Supporting Information Available: Complete tables of crystallographic data, positional parameters, thermal displacement parameters, bond lengths and angles, and intermolecular nonbonding distances for **2**; selected regions of the one-dimensional ^{1}H NMR spectra of **I**, **II** and **III** (Figures S1 and S2); molecular modeling procedures for **III** and listing of newly introduced force field parameters. This material is available free of charge via the Internet at http://pubs.acs.org.

IC991259P

(47) The model based on molecular mechanics calculations (point minimization at $T = 0$ K) does not reflect the dynamic properties of **III** suggested by the NMR data but represents one energetically favored local minimum conformation.

(48) (a) Pil, P. M.; Lippard, S. J. *Science*, **1992**, *256*, 234. (b) Zamble, D. B.; Mu, D.; Reardon, J. T.; Sancar, A.; Lippard, S. J. *Biochemistry* **1996**, *35*, 10004.

(49) Bauer, C.; Preleg-Shulman, T.; Gibson, D.; Wang, H. *Eur. J. Biochem.* **1998**, *256*, 253.

(50) Montine, T. J.; Borch, R. F. *Biochem. Pharmacol*. **1990**, *39*, 1751.